

K-Shell Internal Ionization Accompanying Beta Decay

Yasuhito Isozumi and Sakae Shimizu

Radioisotope Research Center, Kyoto University, Kyoto, Japan

(Received 19 February 1971)

Internal ionization in the K shell during nuclear β decay has been studied experimentally as well as theoretically. The subsequent K x rays were measured in coincidence with emitted electrons for various segments of the β spectra of ^{147}Pm and ^{63}Ni , using 4π detection geometry for these electrons; the sources were mounted in the electron detectors. The energy-dependent ionization probability $P_K(E_\beta^0)$ was measured as a function of E_β^0 , where the parameter E_β^0 is defined as a sum of energies of the β particle and emitted K electron plus the K -shell binding energy of the daughter atom. This energy-dependent and the simultaneously measured total ionization probabilities have been found to be in fairly good agreement with theoretical values calculated by the theory developed based on a relativistic one-step treatment of electron shakeoff. From this result it has been established that electron shakeoff is the predominant mechanism even for electrons (β particles and K electrons) emitted with very low energies. As to the total ionization probability, it is pointed out that the theoretical values calculated by the simple wave-function-overlap theory using self-consistent-field wave functions should be improved by multiplying by a correction factor, a function of B_K and E_0 , where B_K is the K -shell binding energy of the daughter atom and E_0 is the ordinary maximum kinetic energy of β rays. The theoretical treatment of the phenomenon and future fruitful experiments to be hoped for are also discussed.

I. INTRODUCTION

When a radioactive nucleus disintegrates through β decay, shell electrons of that atom may be excited to an unoccupied level, or ionized to the continuum by either the sudden change in nuclear charge (electron shakeoff) or simply by direct collision between the β particle and shell electrons. This phenomenon, so-called internal ionization of shell electrons accompanying β decay, was first investigated theoretically by Feinberg¹ and Migdal² in 1941. The first experimental evidence was established by Boehm and Wu³ by measuring the characteristic x rays in the β decay of ^{147}Pm and ^{210}Bi in 1954. Since these early works a number of experimental workers³⁻⁷ have measured the total probability per β decay of this ionization process using several single- β -decay nuclides. It was concluded from its experimental Z dependence that electron shakeoff may be mainly responsible for the process. On the other hand, by the observation of spectra of low-energy electrons accompanying β decay, Suzor and Charpak⁸ and Spighele and Suzor⁹ claimed that there was a serious disagreement with the theory of electron shakeoff. Their works stimulated Feinberg¹⁰ and Weiner¹¹ to reexamine the mechanism of internal ionization. They suggested that, for the K shell, direct collision should also be taken into consideration as one of important possible processes. Erman *et al.*¹² and Stephan and Crasemann^{13, 14} have measured the β energy dependence of the

probability for the K shell.

In these works for the K shell, because of the experimental arrangement of a β -ray source always placed between two detectors, one for K x rays and the other for both β particles and emitted K electrons, coincidences were measured both between K x rays and β particles and between K x rays and emitted K electrons, i.e., the composite (emitted K electrons and β particles) electron spectra in coincidence with K x rays were measured but not in the low-energy region of β decay. Recently, Fischbeck *et al.*¹⁵ have performed a similar experiment to observe the precise composite electron spectrum of ^{143}Pr even in the low-energy region with the aid of a magnetic-lens spectrometer. All of them concluded that electron shakeoff is the main process for the phenomenon.

In the present paper, we report details of our experimental work with ^{147}Pm and ^{63}Ni using improved detection systems with the intention of providing additional information on this phenomenon in the whole energy region of β decay by proposing a new concept of β energy dependence of the probability. Since no exact observations have been published, especially in the low-energy region, careful procedures have been pursued to obtain information in this region. A refined theoretical treatment reconciled with the experimental results has also been studied with the aim of throwing light on our understanding of the K -shell internal ionization during β decay.

II. PRINCIPLE OF THE MEASUREMENT

When internal ionization in the K shell occurs during β decay, a β particle and a neutrino are emitted from the nucleus and also a K electron from its orbit, followed immediately by emission of a K x ray with a certain probability defined by the K -shell fluorescence yield. Denoting the maximum kinetic energy of the continuous β -ray spectrum of ordinary β decay by E_0 , we can express the energetics for K -shell internal ionization by

$$E_0 = E_\beta + E_\nu + E_K + B_K, \quad (1)$$

where E_β , E_ν , and E_K are the kinetic energies of β particle, neutrino, and emitted K electron, respectively, and B_K is the K -shell binding energy of the daughter atom.

In the present experiment the β -ray source is mounted inside the electron detector to achieve 4π detection geometry. Thus, when the phenomenon to be studied takes place a sum of energies of the β particle and K electron emitted simultaneously, $E_\beta + E_K$, is measured in coincidence with an emitted K x ray. In the present work, from the experimental data we can easily derive the probability of the phenomenon as a function of the sum of energies $E_\beta^0 \equiv E_\beta + E_K + B_K$, even in the low-energy region of the coincidence electron spectrum.

We present a rationale for the use of the energy E_β^0 . This would be defined as the initial energy of a β particle if the K -shell internal ionization were assumed to take place through two steps, viz., the ordinary β decay first occurs by emission of a β particle with an energy E_β^0 and a neutrino with an energy $E_0 - E_\beta^0$, and then a K electron is ejected with a kinetic energy E_K by an interaction with the β particle. But, as is well known, electron shake-off occurs by a one-step process, where three leptons (β particle, K electron, and neutrino) are emitted simultaneously. Although the term "initial β energy" may be understood to imply a two-step process, such is not our intention; nevertheless we did employ the energy E_β^0 as a convenient parameter of the energy-dependent probability. It should be noted that in the present work we never treat the phenomenon as a two-step process. As it is discussed in Secs. V and VI, the definition of the ionization probability using the energy E_β^0 is more helpful for understanding the mechanism of K -shell internal ionization than that using other parameters such as E_β or $E_\beta + E_K$ or $E_\beta + B_K$.

The photon spectra were observed by the x-ray detector in coincidence with pulses from the electron channel corresponding to the selected energy sum of β particle and emitted K electron, $E_\beta + E_K$. The ionization probability per β decay as a func-

tion of E_β^0 can be given by

$$P_K(E_\beta^0) = \frac{N_x(E_\beta^0)}{N(E_\beta + E_K)} \frac{n(E_\beta + E_K)}{n(E_\beta^0)} \frac{1}{D\omega_K}, \quad (2)$$

where $N(E_\beta + E_K)$ is the observed counting rate from the electron detector with an energy selection of $E_\beta + E_K$, $N_x(E_\beta^0)$ is the counting rate of the K x-ray peak in the observed coincident photon spectrum, D is the effective detection efficiency of the x-ray detector, and ω_K is the K fluorescence yield of the daughter atom. In this expression the second factor, $n(E_\beta + E_K)/n(E_\beta^0)$, is a correction for $N(E_\beta + E_K)$; $n(E_\beta + E_K)$ and $n(E_\beta^0)$ are the singles counting rates of the β -ray spectrum at energies $E_\beta + E_K$ and E_β^0 , respectively, measured by the electron detector having the β -ray source inside it. This procedure for correcting $N(E_\beta + E_K)$ by the use of the observed value of $n(E_\beta + E_K)/n(E_\beta^0)$ is essential in the present work to estimate the ionization probability per β decay as a function of E_β^0 .

In the present work the total ionization probability per β decay, \bar{P}_K , is defined as that for all β particles with energies larger than B_K . \bar{P}_K can be given simply by

$$\bar{P}_K = \frac{N_x}{N_\beta} \frac{n(\geq 0)}{n(\geq B_K)} \frac{1}{D\omega_K}, \quad (3)$$

where N_β is the observed counting rate for electrons with energies above zero and N_x that of the coincident K x rays, and $n(\geq 0)$ and $n(\geq B_K)$ are the counting rates of all β particles with kinetic energies above zero and B_K , respectively. It is noted that \bar{P}_K given by this expression is different from the experimental total ionization probability P_K defined by other workers, except Erman *et al.*¹² with respect to the term $n(\geq 0)/n(\geq B_K)$. Fuller discussion on this point is given in Secs. V and VI.

III. EXPERIMENTAL PROCEDURE

In the present work β -ray emitters ^{147}Pm and ^{63}Ni were chosen, because the relatively large values of B_K/E_0 are advantageous for observing the phenomenon in the low-energy region of β spectra; $E_0 = 225$ keV and $B_K = 47$ keV for ^{147}Pm , and $E_0 = 67$ keV and $B_K = 9.0$ keV for ^{63}Ni . The nuclide ^{63}Ni has been shown to decay to the ground state of ^{63}Cu through a pure single β decay, while ^{147}Pm decays mainly to the ground state of ^{147}Sm through β decay but with a very weak β branch to the 122-keV first excited level of ^{147}Sm .¹⁶ The branching ratio of this weak β decay, determined by us as $(5.1 \pm 1.0) \times 10^{-5}$, had to be taken into account in the present work with ^{147}Pm , as mentioned in Sec. IV.

A. Apparatus for the Experiment with ^{147}Pm

A split anthracene crystal was used as an electron detector. An anthracene crystal of 8-mm diam by 4-mm thickness was cut into two pieces at its center line. The residuum of a drop of $^{147}\text{PmCl}_3$ solution of about 1 mm in diameter was sandwiched between sliced surfaces of these two pieces to achieve 4π detection geometry. This split crystal holding the ^{147}Pm source was covered with a thin aluminum reflector and then mounted on a Toshiba 7696 photomultiplier with a special coupling material (G.E. TRV-602 silicone potting compound). The intensity of this source was estimated to be about $0.6 \mu\text{Ci}$.

The 40-keV Sm K x rays emitted from the source by the process to be studied were detected by a 38-mm-diam by 6.0-mm-thick NaI(Tl) detector. Both detectors were housed in a brass tube. The experimental assembly of the detectors and source is shown in Fig. 1.

The light output from the anthracene crystal is known to have a negative temperature coefficient. Since the coefficient of the crystal used in the present work was found to be $-0.7\%/^{\circ}\text{C}$ near room temperature, and long-run measurements had to be performed for several months, the whole assembly of the detectors was installed in a special beer refrigerator to keep the temperature of the crystal constant, at $4.0 \pm 0.3^{\circ}\text{C}$ during the experiment.

The Kurie plot of β rays from ^{147}Pm (once parity forbidden) obtained by the present device using a split anthracene crystal was found to be linear from 30 keV to the end point of 225 keV, while when the source was placed just above a single crystal of the same dimensions the plot was linear

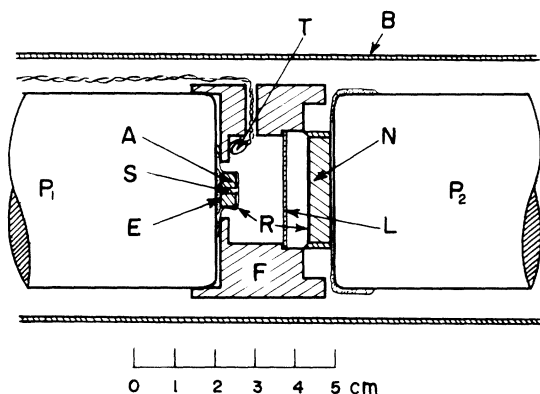


FIG. 1. Experimental arrangement of x-ray and electron detectors and ^{147}Pm source: A, split anthracene crystal; N, NaI(Tl) crystal; S, ^{147}Pm source; E, G.E. TRV-602 silicone potting compound; R, aluminum reflectors; L, Lucite plate; P₁ and P₂, Toshiba 7696 photomultipliers; T, thermistor; F, Lucite frame; B, brass tube.

from about 110 keV. This favorable result is due to the fact that the effect of backscattering of β particles from the surface of the crystal can be eliminated by the use of the sandwich method.

The coincidence circuit connecting both detector channels including the DD-2 amplifiers and single-channel analyzers was a conventional fast-slow coincidence unit with a time resolution $2\tau = 180$ nsec, which was rather poor, but in the present experiment the ratio of the random to true coincidences was found to be about 1/30 with the $0.6\text{-}\mu\text{Ci}$ ^{147}Pm source. The pulses from the coincidence unit triggered a multichannel pulse-height analyzer to record the x-ray spectrum.

Since the stability of the whole system was crucial to the success of the experiment, before long-run measurements the drift of the system was examined carefully using a ^{137}Cs source; the spectrum of the 32-keV Ba K x rays was observed in coincidence with the 624-keV K conversion electrons. The fluctuation in stability of the whole system was found to be less than 1% for two weeks. Such a satisfactory stability could be achieved by installing the detector assembly inside the refrigerator.

B. Apparatus for the Experiment with ^{63}Ni

Since E_0 of the β rays of ^{63}Ni is only 67 keV, to achieve 4π detection geometry a gas-flow proportional tube counter (30 cm long by 10-cm i.d.) was used as an electron detector, inside of which a ^{63}Ni source was mounted. For detection of the 8.1-keV Cu K x rays from the source, another gas-flow proportional tube counter (30 cm long by 5-cm i.d.) was constructed. Aluminum was chosen as the wall material of these counters to avoid possible emission of undesirable x rays near 8 keV from the counter wall, which may be observed when copper or brass or iron is used. The counter gas (90% Ar-10% CH_4 mixture) at 1 atm was flowed through the counters at a constant rate of about 1 cc/min. The side windows of both counters were covered by a very thin Mylar film ($1 \text{ mg}/\text{cm}^2$), on which about 200- \AA -thick aluminum was evaporated.

One drop of $^{63}\text{NiCl}_2$ solution was evaporated to a residuum of about 3 mm in diam on a water-spread Formvar film ($\approx 2 \mu\text{g}/\text{cm}^2$) supported by a 5-mm-diam ring frame of a 90- μ tungsten wire. The intensity of this very thin source was estimated to be about $0.3 \mu\text{Ci}$. The source frame was fastened to the end of a Lucite bar and then inserted into the electron counter through a side hole so that the distance from the source to the window was set as to be about 30 mm and the source-supporting film was perpendicular to the

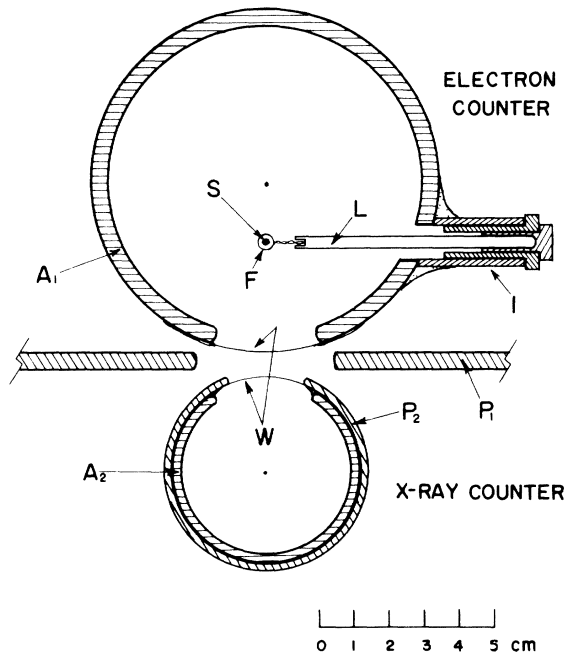


FIG. 2. Experimental arrangement of x-ray and electron proportional counters: A_1 and A_2 , aluminum counter cylinders; S, ^{63}Ni source; F, Formvar film; L, Lucite bar; I, source inlet; W, aluminum-evaporated Mylar windows; P_1 , lead plate; P_2 , lead cover.

center wire. The 3-cm gas path to the window was enough to absorb all β particles from the ^{63}Ni source. Moreover, most of the 8.1-keV photons to be observed by the x-ray counter could escape from the electron counter, since only 29.6% was found to be absorbed in the 3-cm-thick gas layer. The experimental arrangement of the electron counter with the ^{63}Ni source in it and the x-ray counter is shown in Fig. 2. A 2-mm-thick lead sheet surrounding the x-ray counter served to limit the opening of the window exactly for the x rays to be measured. A 5-mm-thick lead plate, shown in the figure, was used to reduce the natural background in the coincidence measurement. Many precautions were taken against fluctuation of the applied voltage and change in the flow rate of the counter gas. The drifts of the gains from the counters could be kept less than about 3% during the coincidence experiment for about five months.

The β -ray spectrum of ^{63}Ni (l forbidden) was measured with the same arrangement with the inserted source as that mentioned above. Since the shape of the low-energy region of the spectrum was found to depend strongly on the preparation procedure of the source residuum, the greatest possible precaution was paid to eliminate dust and moisture, which appeared to be harmful to

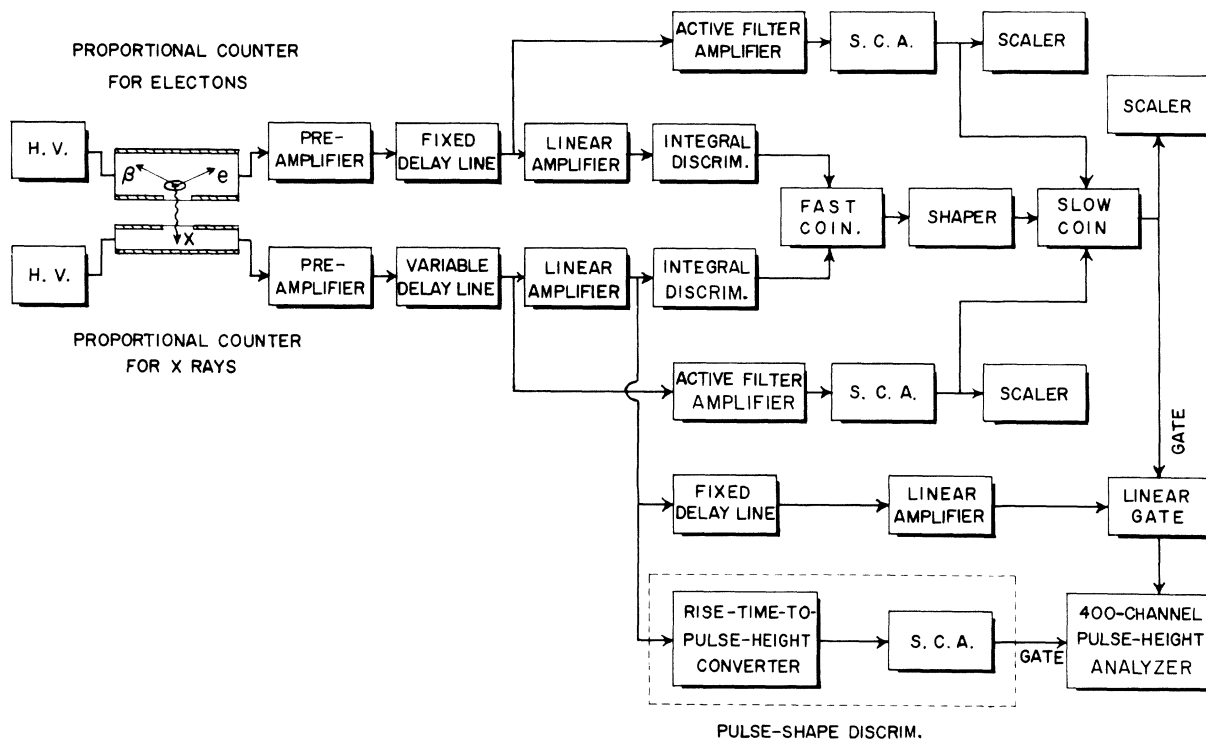


FIG. 3. Block diagram of the electronic system used in the coincidence experiment with ^{63}Ni .

obtaining a reliable spectrum. The best source, judged by examining the shape of the whole spectrum obtained, was used in the present experiment.

A block diagram of the electronic system is schematically shown in Fig. 3. The electronics is composed of two circuits; one is a fast-slow coincidence unit and the other is a pulse-shape-discriminator (PSD) unit built in the x-ray channel, which serves to eliminate a large number of false coincidences caused by cosmic rays and natural γ rays.

The coincidence unit was designed by taking account of unavoidable defects inherent in the gas proportional counter. In the present circuit, in order to obtain better time resolution of the coincidence unit, a leading-edge timing method rather than a conventional crossover method was adopted to pick off the timing of the event. The resolving time of our coincidence unit was about $1.8 \mu\text{sec}$. In the present experiment, even with such a poor resolving time, the ratio of the random to true coincidences was found to be about $\frac{1}{20}$.

Since in the present experiment two gas proportional tube counters with quite large sensitive volumes were employed, false coincidences by high-energy cosmic rays and natural γ -ray background were inevitable. In order to eliminate such false coincidences an electronic device has been developed which discriminated incident radiations by means of their pulse shapes from the detectors. Similar electronics has recently been applied to measurements of low-energy cosmic

x rays by the use of gas proportional counters.¹⁷ We adapted this method to use with two proportional counters in a coincidence arrangement.¹⁸ Our PSD built in the x-ray channel is composed of a risetime-to-pulse-height converter and a single-channel analyzer (see Fig. 3). Reduction in the number of the x-ray signals by the use of the PSD circuit was found to be less than 5%. In Fig. 4 are shown the photon spectra obtained in coincidence with electrons from a ^{63}Ni source with and without the use of the PSD. Only when this device was used can a small x-ray peak due to K-shell internal ionization in β decay of ^{63}Ni be recognized clearly, while without it the peak is buried completely in the large background of false coincidences. This PSD circuit was an indispensable aid in the present coincidence experiment using two proportional counters.

C. Measurements

In order to estimate $P_K(E_\beta^0)$ defined by Eq. (2), the photon spectra in coincidence with electrons having a selected energy range were observed by means of the previously described measuring systems. The energy region of the β -ray spectrum was divided into seven segments in both the ^{147}Pm and ^{63}Ni cases. Each segment was selected by adjusting the window of the single-channel analyzer in the electron channel. Considering the gradual decrease in number of electrons in the higher-energy region of the spectrum, the window was made wider for electrons with higher energies. When we measured the total ionization probability per β decay in the case of ^{147}Pm , the window was set so as to cover electron energies from 25 keV to the maximum β -ray energy, 225 keV, while in the case of ^{63}Ni , from 3 keV to the maximum β -ray energy, 67 keV. These lower limits of the window setting were necessary to eliminate noise from the electronics. The coincidence efficiency was believed to be about 100%, almost independent of selection of the energy segment. It was confirmed by the fact that no appreciable change in the coincidence counts was observed when the gain of the linear amplifier in the electron channel was considerably shifted. During each experimental run, the counting rates of both electron and x-ray channels, the β spectra, the coincident photon spectra, and the coincidence cable curves were measured every 12 h in order to monitor performance of the whole measuring system.

Some typical spectra of photons from a ^{147}Pm and a ^{63}Ni source, observed in coincidence with pulses from the electron channel, are shown in Figs. 5 and 6, respectively. As is understood

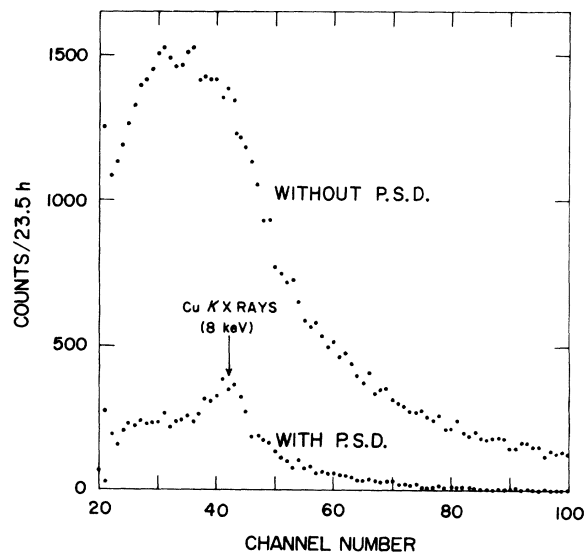


FIG. 4. Photon spectra in coincidence with electrons emitted from the ^{63}Ni source obtained with and without the use of a pulse-shape discriminator (PSD) in the x-ray channel.

from the decay scheme of ^{147}Pm shown in Fig. 7, when the electron channel selects energies less than 103 keV, there appear two evident peaks in the photon channel; one at 40 keV due to the K x rays in question from the daughter atom, Sm, and the other in the vicinity of 120 keV caused by γ rays from the transition from the 122-keV first excited level of ^{147}Sm to its ground state. Since 40-keV x rays may also be emitted after K conversion of this transition, the observed peak must be corrected to evaluate the contribution only from the process to be studied here; details of this correction procedure are discussed in the following section. The spectra with ^{63}Ni show also two evident peaks, one at 8 keV due to K x rays from the daughter atom, Cu, and the other due to the 3.0-keV Ar K x rays from ionization of the counter gas by β particles. The continuous backgrounds in all observed spectra are due to the internal and external bremsstrahlung photons from the source and its surroundings. With the present arrangement of the source it was very difficult to suppress the background further.

D. Detection Efficiency of the X-Ray Detectors

The effective detection efficiency, D in Eqs. (2)

and (3), of the x-ray detectors must be evaluated for the present experimental arrangement; D_s of the thin NaI(Tl) detector for the 40-keV x rays and the 122-keV γ rays, and D_p of the gas proportional counter with a definite side window for the 8.1-keV x rays.

For the thin NaI(Tl) detector used in the case of ^{147}Pm , D_s can be given by the following expression:

$$D_s = D_0 R a_1 a_2 a_3 / (1 + g). \quad (4)$$

The symbols in the expression are: D_0 is the detection efficiency for the photons to be detected; R is the peak-to-total ratio; g is the correction factor for the escape peak of the IK x rays; and a_1 , a_2 , a_3 are the correction factors for absorption of the photons in the anthracene crystal, Lucite absorber between both scintillation detectors (see Fig. 1), and the aluminum reflector foils on the NaI(Tl) and anthracene crystals, respectively.

The detection efficiency D_0 could be calculated easily by the common procedure adopted by other workers¹⁹ using numerical values of the dimensions of the NaI(Tl) crystal, distance from the source to the crystal, and the linear attenuation

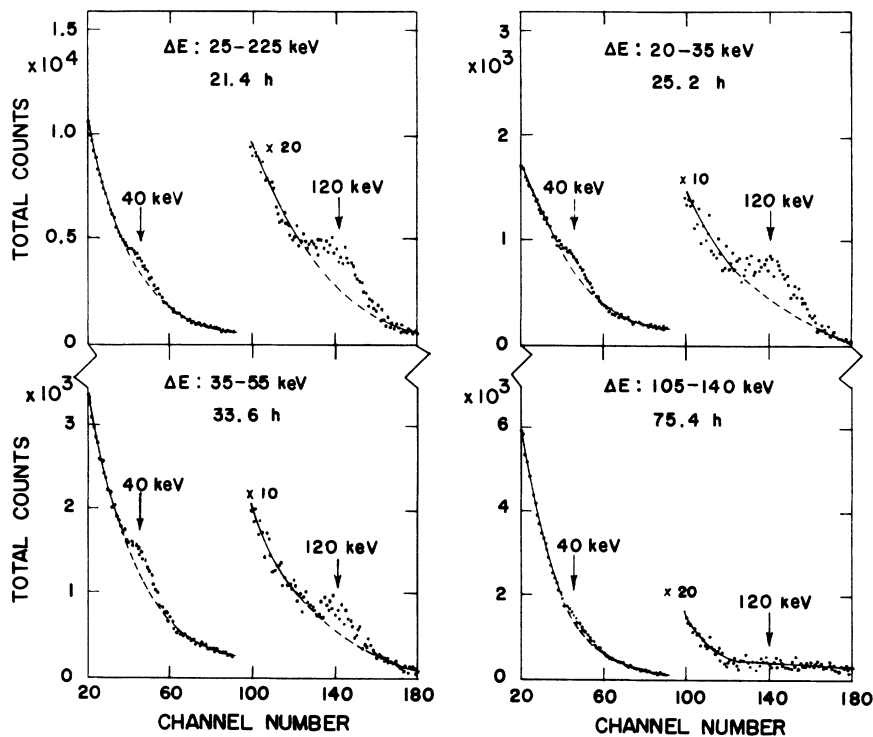


FIG. 5. Photon spectra from the ^{147}Pm source observed in coincidence with electrons emitted from the source. ΔE is the electron-channel window width selected. The 40-keV Sm K x rays resulting mainly from the K -shell internal ionization are superimposed on the bremsstrahlung spectra. The 120-keV peak observed for electrons below 103 keV is due to the very weak γ rays caused by the transition from the 122-keV first excited level of ^{147}Sm to its ground state (see Fig. 7).

coefficient of the photon in the crystal. The value of R was calculated by the Monte Carlo method developed by Miller, Reynolds, and Snow.²⁰ The correction factors a_1 , a_2 , and a_3 were evaluated for the present arrangement by utilizing the numerical values of the γ -ray attenuation coefficients given in the table prepared by Davisson.²¹ The correction factor g was estimated by interpolation of the values provided by Dell and Ebert²²; 0.24 for the 40-keV photons and ≈ 0.00 for the 122-keV photons. The numerical values of D_s thus estimated and adopted for the present experimental geometry are as follows: $D_s = (9.42 \pm 0.51) \times 10^{-2}$ for the 40-keV photons, and $D_s = (8.67 \pm 0.56) \times 10^{-2}$ for the 122-keV photons.

In the case with ^{63}Ni , the effective detection efficiency, D_p , of the gas proportional counter used for x-ray detection was evaluated by pursuing the following rather complicated procedure. This can be given by

$$D_p = D'_0 a'_1 a'_2 / (1 + g'), \quad (5)$$

where D'_0 is the detection efficiency for the 8.1-keV photon, provided that there is no material between the source and the x-ray counter, a'_1 is the correction factor for the absorption of the x rays in gas in the electron counter, a'_2 is that for the Mylar window of the electron counter and air between both counters, and g' is a correction factor for the escape peak at about 5 keV due to the Ar K x rays. The detection efficiency D'_0 was determined by making use of the NaI(Tl) crystal, whose diameter was chosen to be the same as the opening of the side window of the x-ray proportional counter, viz., a crystal of 25-mm diam by 4-mm thickness. A ^{65}Zn source of about 100 μCi was mounted in the electron proportional counter. The geometrical arrangement of the source mounting was quite similar to that in the actual experiment with ^{63}Ni . First, the 8.1-keV Cu K x rays from the ^{65}Zn source were measured with the x-ray proportional counter in the actual geometrical arrangement, then this counter was removed and the NaI(Tl) crystal detector was installed so that its surface

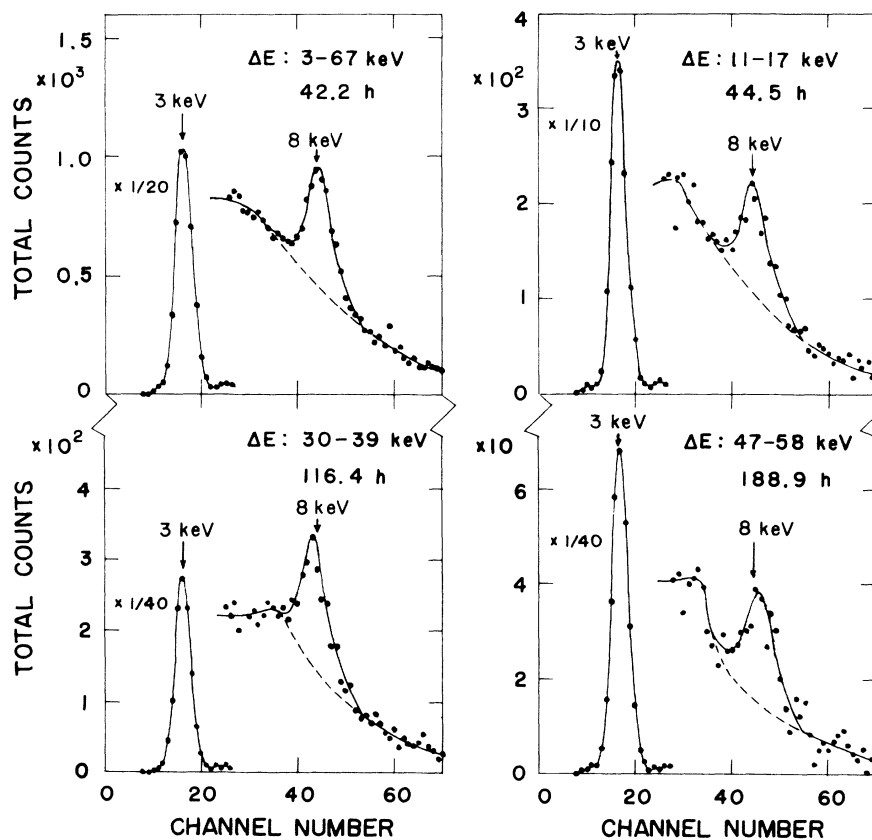


FIG. 6. Photon spectra from the ^{63}Ni source observed in coincidence with electrons emitted from the source. ΔE is the electron-channel window width selected. The 8-keV Cu K x rays resulting from the K -shell internal ionization are superimposed on the bremsstrahlung spectra. An evident peak at 3 keV is due to the Ar K x rays from ionization of the counter gas by β particles.

was located at the same position as the Mylar window of the x-ray counter. When the former counter gives the counting rate N_p and the latter gives N_s , D'_0 in Eq. (5) can be given very approximately by

$$D'_0 = D'_s N_p / N_s, \quad (6)$$

where D'_s is the detection efficiency of this NaI(Tl) crystal. The absorption of the x rays in a beryllium foil ($\sim 200 \mu$) on the crystal was found to be negligible. The value of D'_s was calculated by a procedure similar to that for D_0 in Eq. (4) as mentioned above. Thus, D'_0 was obtained as to be $(2.41 \pm 0.23) \times 10^{-2}$. The error is mainly due to an uncertainty in the distance from the source to the surface of the crystal detector. In order to determine a'_1 in Eq. (5) experimentally, the counter gas in the electron counter was replaced with hydrogen of 1 atm. Since the x rays concerned are scarcely absorbed in hydrogen, a'_1 can be given by

$$a'_1 = N_p / N_H, \quad (7)$$

where N_p is the counting rate of the x rays measured by the x-ray counter, and N_H is that by the same counter but with the electron counter filled with hydrogen. An estimated value of a'_1 was 0.704 ± 0.005 . The factor a'_2 was also estimated from Davisson's table²¹: $a'_2 = 0.99$. The correction factor g' could be estimated from the spectrum of the 8.1-keV x rays from ^{65}Zn measured by our x-ray counter: $g' = 0.078 \pm 0.001$. From these results the effective detection efficiency of the x-ray counter was determined to be $D_p = (1.56 \pm 0.15) \times 10^{-2}$ for the 8.1-keV photons.

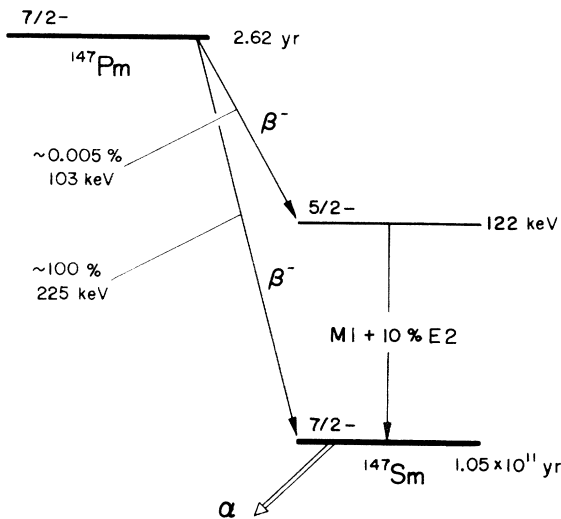


FIG. 7. Decay scheme of ^{147}Pm .

E. K-Shell Fluorescence Yields

As the most reliable values for the K-shell fluorescence yield ω_K in Eqs. (2) and (3), we used the data recently provided by Kostroun, Chen, and Crasemann.²³ The numerical values we adopted are as follows: $\omega_K = 0.93$ for ^{62}Sm , and $\omega_K = 0.45$ for ^{29}Cu .

IV. EXPERIMENTAL RESULTS

Except for the factors $n(E_\beta + E_K)/n(E_\beta^0)$ in Eq. (2) for $P_K(E_\beta^0)$, and $n(\geq 0)/n(\geq B_K)$ in Eq. (3) for \bar{P}_K , all other terms in these equations were determined as described in the preceding section. In the β -ray spectrum of both ^{147}Pm and ^{63}Ni , observed by the electron detector containing the source, the ratio of the counting rate in the β -energy region for $E_\beta + E_K$ to that in the region for $E_\beta^0 = E_\beta + E_K + B_K$ was adopted as the correction factor $n(E_\beta + E_K)/n(E_\beta^0)$. The factor $n(\geq 0)/n(\geq B_K)$ could also be evaluated approximately from the ratio of the counting rate of all β particles above the lower discriminator level (25 keV for ^{147}Pm and 3 keV for ^{63}Ni) to that of β particles with energies larger than B_K in the β -ray spectrum.

For the electron detectors used in the present work, in addition to the energies of the β particle and ejected K electron, simultaneously emitted L x rays and/or Auger electrons are detected.²⁴ To account for the additional absorption of this small energy ($\approx B_L$) in the electron detector, only about 5 keV for ^{147}Pm and 1 keV for ^{63}Ni , $P_K(E_\beta^0)$ given by Eq. (2), and \bar{P}_K by Eq. (3) must be slightly modified, viz., Eqs. (2) and (3) were multiplied by factors $n(E_\beta + E_K + B_L)/n(E_\beta + E_K)$ and $n(\geq B_L)/n(\geq 0)$, respectively, where B_L is the L binding energy of the daughter atom. When we estimated $P_K(E_\beta^0)$ and \bar{P}_K experimentally using Eqs. (2) and (3), such correction factors were taken into account.

In the experiment with ^{147}Pm , a correction should be made for the minute contribution to the observed x-ray peak, which is caused by K internal conversion from the 122-keV first excited level of ^{147}Sm to its ground state, as mentioned in Sec. III C. Since the energy of this K conversion electron is 75 keV ($= 122 \text{ keV} - B_K$) and ^{147}Pm decays according to the scheme as shown in Fig. 7, when the energy window of the electron channel is set in the region lying between 75 and 178 keV ($= E_0 - B_K$), the contribution only from the x rays due to K-shell internal ionization, $N_x^0(E_\beta^0)$, can be expressed by

$$N_x^0(E_\beta^0) = \frac{N_x(E_\beta^0)}{D_{40}} - \alpha_K \frac{N_\gamma(E_\beta + E_K - 75 \text{ keV})}{D_{122}}, \quad (8)$$

where α_K is the K -shell conversion coefficient of the transition concerned, D_{40} and D_{122} are the effective detection efficiencies of the x-ray detector for the 40-keV x rays and 122-keV γ rays, respectively, and $N_{\gamma(E_{\beta}+E_K-75 \text{ keV})}$ is the counting rate of the observed 122-keV γ -ray peak when the electron window is set at $E_{\beta}+E_K-75$ keV. Therefore, $P_K(E_{\beta}^0)$ for ^{147}Pm can be obtained by replacing $N_x(E_{\beta}^0)$ in Eq. (2) with the right-hand side of Eq. (8) as

$$P_K(E_{\beta}^0) = \frac{N_x(E_{\beta}^0)}{N(E_{\beta}+E_K)} \frac{n(E_{\beta}+E_K)}{n(E_{\beta}^0)} \frac{1}{D_{40}\omega_K} \times \left[1 - \alpha_K \frac{N_{\gamma(E_{\beta}+E_K-75 \text{ keV})}}{N_x(E_{\beta}^0)} \frac{D_{40}}{D_{122}} \right]. \quad (9)$$

The last term can be regarded as a correction factor for the effect of the K internal conversion involved. The expression [Eq. (3)] for the total ionization probability per β decay should also be corrected by this factor. As a numerical value of α_K , we adopted 1.05 ± 0.06 determined by Schwerdtfeger, Prask, and Mihelich.²⁵

The experimental values of the probability $P_K(E_{\beta}^0)$ obtained by the present work for ^{147}Pm and ^{63}Ni are shown by open circles in Figs. 8 and 9, respectively. The total ionization probability \bar{P}_K is also given in the figures. The errors shown are due to those of counting statistics, uncertainty in the shape of the continuous background under the observed x-ray peaks in the photon spectra, and uncertainties in factors in Eqs. (2), (3), and (8). The horizontal bars indicate the width of the

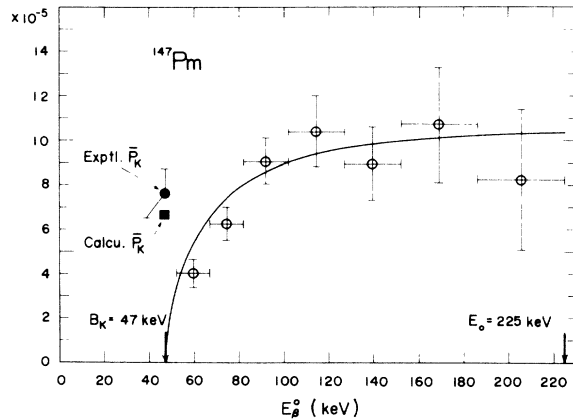


FIG. 8. Measured energy-dependent K -shell internal ionization probability $P_K(E_{\beta}^0)$ for ^{147}Pm . Horizontal bars indicate the electron-channel window in coincidence measurements and vertical bars represent standard deviations. The solid curve represents the theoretical curve calculated by Eq. (13), based on the one-step electron shakeoff treatment. Measured total ionization probability \bar{P}_K and its theoretical value calculated by Eq. (14) are also shown.

electron-channel window selected in each coincidence measurement. The data at the lowest E_{β}^0 in both figures may be less reliable than indicated by the error bars, since in this energy region β spectra were rather distorted by suspicious noises caused by interaction between β particles and surroundings near the β -ray source. It is seen from these figures that the probability $P_K(E_{\beta}^0)$ for both ^{147}Pm and ^{63}Ni is almost independent of the energy E_{β}^0 in the higher-energy region of the spectra above twice the K binding energy, B_K , of the daughter atom involved, but it drops rather steeply in the region below about $E_{\beta}^0 = 2B_K$, especially for ^{147}Pm . However, we must add that, in the case of ^{63}Ni , if a source thinner than that used could be prepared, more refined data would be obtained in the low-energy region. Physical meanings of such a trend are discussed in Sec. VI.

V. THEORETICAL TREATMENT

As mentioned in Sec. II, electron shakeoff occurs by a one-step process. This means that the kinetic energy of the ejected K electron, E_K , is given by an energy sharing among all three leptons, including the neutrino. Both the E_{β}^0 -dependent probability $P_K(E_{\beta}^0)$ and the total ionization probability \bar{P}_K defined in the present work should also be evaluated by a one-step treatment.

Stephas and Crasemann^{13, 14} have developed the

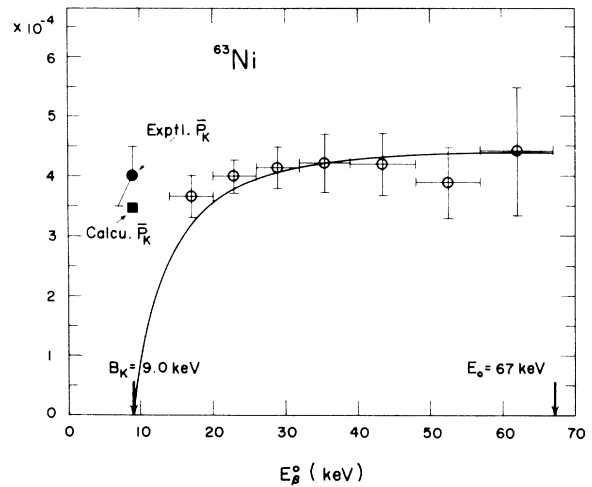


FIG. 9. Measured energy-dependent K -shell internal ionization probability $P_K(E_{\beta}^0)$ for ^{63}Ni . Horizontal bars indicate the electron-channel window in coincidence measurements and vertical bars represent standard deviations. The solid curve represents the theoretical curve calculated by Eq. (13), based on the one-step electron shakeoff treatment. Measured total ionization probability \bar{P}_K and its theoretical value calculated by Eq. (14) are also shown.

theory of the electron shakeoff as a one-step process. They have defined a probability $P_K(E_\beta)$ as a function of the energy of the β particle, E_β . However, since in their experiment the composite electron spectrum (emitted K electrons plus β particles) in coincidence with K x rays was observed, $P_K(E_\beta) + P_K(E_K)$ had to be compared with the experimental data. In the present work, a sum of energies of β particle and emitted K electron in coincidence with a K x ray was measured. The 4π detection for electrons ensured the measurement even when both β particle and emitted K electron have very low energies. We employed E_β^0 ($\equiv E_\beta + E_K + B_K$) as a parameter of the energy-dependent probability. There is no connection between the energy of a β particle emitted from ordinary β decay and E_β or E_β^0 in the electron shakeoff during β decay. Any of all possible parameters, E_β , E_β^0 , $E_\beta + E_K$, or $E_\beta + B_K$, can be

understood only as a convenient parameter in order to compare the experiment with the theory. Nevertheless, we adopted a parameter E_β^0 by reflecting upon the fact that this energy is equal to the initial β energy in a two-step treatment and if the shakeoff occurs through a two-step process, $P_K(E_\beta^0)$ should be independent of E_β^0 in the whole energy region.¹²

$P_K(E_\beta^0)$ can be easily derived based upon the theory of the phenomenon as a one-step process, developed by Stepas and Crasemann.^{13, 14} If an atom undergoes β decay, a K -shell electron can also be ejected from an eigenstate of the parent atom, $\psi_i(Z, K)$, into a continuum of the daughter, $\psi_f(Z+1, E_K)$, with kinetic energy E_K , under the sudden change of the nuclear charge from Z to $Z+1$. Then, the differential transition probability for the electron shakeoff process can be expressed as

$$dW_K = \frac{2\pi}{\hbar} |\langle \psi_f(Z+1; e, \beta) \psi_f(N) | H_B | \psi_i(N) \psi_\nu \psi_i(Z, K) \rangle|^2 \rho(\beta, \nu, e), \quad (10)$$

where $\psi_i(N)$ and $\psi_f(N)$ are the initial and final nuclear wave functions, $\psi_f(Z+1; e, \beta)$ the antisymmetric wave function for the β particle and K electron, ψ_ν the neutrino wave function, H_B the weak interaction Hamiltonian, and $\rho(\beta, \nu, e)$ the density of final states for β particle, neutrino, and emitted K electron. It should be noted that the expression treats β decay as a transition of the atom as a whole, including atomic variables in both final and initial states.

Upon integrating Eq. (10) over the neutrino energy E_ν , we obtain

$$W_K(E_\beta, E_K) dE_\beta dE_K = 2eA |M_N|^2 S(E_\beta, E_0 - E_\beta^0) F(Z+1, E_\beta) |M_A|^2 p_B(E_\beta + 1) (E_0 - E_\beta^0)^2 dE_\beta dE_K. \quad (11)$$

In this expression, A is a constant factor equal to $(m^5 c^4 g^2 / \hbar^7) (1/2\pi^3)$ provided all other factors are dimensionless, where m , c , and g are the rest mass of the electron, light velocity, and the coupling constant of the weak interaction, respectively. M_N is the energy-independent part of the nuclear matrix element, $S(E_\beta, E_0 - E_\beta^0)$ is the energy-dependent shape factor for the electron shakeoff, $F(Z+1, E_\beta)$ is the Coulomb correction factor, the factor e arises from the antisymmetrization of the final electron states of β particle and emitted K electron, a factor 2 accounts for two K electrons, and p_B is the linear momentum for the β particle. M_A is the atomic matrix element given by $\langle \psi_f(Z+1, E_K) | \psi_i(Z, K) \rangle$. In the present calculation we used the analytical form of $|M_A|^2$ obtained by Stepas and Crasemann¹³ using relativistic hydrogenic wave functions for $\psi_f(Z+1, E_K)$ and $\psi_i(Z, K)$. It is noted that a similar expression given by them [see Eq. (2.10) in Ref. 14] differs from our expression [Eq. (11)] by a factor of $(m^3 c^3 / 2\pi^2 \hbar^3) p_K(E_K + 1)$. Their matrix element $|M_A|^2$ is not normalized in momentum space, since $\psi_f(Z+1, E_K)$ is normalized only by the energy $E_K + 1$, not by wave number. Their expression, therefore, should be divided by the factor mentioned above. Fuller discussion on the factor $p_K(E_K + 1)$ has recently been given by Fischbeck *et al.*¹⁵

The absolute transition probability as a function of E_β^0 is obtained by integrating Eq. (11) over E_K after changing the variable E_β to $E_\beta^0 - E_K - B_K$ as

$$\begin{aligned} W_K(E_\beta^0) &= \int_0^{E_\beta^0 - B_K} W_K(E_\beta^0 - E_K - B_K, E_K) dE_K \\ &= 2eA |M_N|^2 \int_0^{E_\beta^0 - B_K} S(E_\beta, E_0 - E_\beta^0) F(Z+1, E_\beta) |M_A|^2 p_B(E_\beta + 1) (E_0 - E_\beta^0)^2 dE_K. \end{aligned} \quad (12)$$

The E_β^0 -dependent probability of the K -electron shakeoff during β decay can be expressed by the following equation:

$$P_K(E_\beta^0) = \frac{W_K(E_\beta^0)}{W_\beta(E_\beta = E_\beta^0)} = 2e \int_0^{E_\beta^0 - B_K} |M_A|^2 \frac{S(E_\beta, E_0 - E_\beta^0)}{S(E_\beta^0, E_0 - E_\beta^0)} \frac{F(Z+1, E_\beta)}{F(Z+1, E_\beta^0)} \left[\frac{E_\beta(E_\beta + 2)}{E_\beta^0(E_\beta^0 + 2)} \right]^{1/2} \left(\frac{E_\beta + 1}{E_\beta^0 + 1} \right) dE_K, \quad (13)$$

where $W_\beta(E_\beta)$ is defined as the absolute transition probability of ordinary β decay. The total ionization probability \bar{P}_K , corresponding to Eq. (3), can also be given by

$$\bar{P}_K = 2\epsilon \frac{\int_{B_K}^{E_0} W_K(E_\beta^0) dE_\beta^0}{\int_{B_K}^{E_0} W_\beta(E_\beta) dE_\beta} = 2\epsilon \frac{\int_{B_K}^{E_0} (E_0 - E_\beta^0)^2 dE_\beta^0 \int_0^{E_\beta^0 - B_K} S(E_\beta, E_0 - E_\beta) F(Z+1, E_\beta) |M_A|^2 p_\beta(E_\beta + 1) dE_K}{\int_{B_K}^{E_0} S(E_\beta, E_0 - E_\beta) F(Z+1, E_\beta) p_\beta(E_\beta + 1) (E_0 - E_\beta)^2 dE_\beta}. \quad (14)$$

We evaluate the probabilities $P_K(E_\beta^0)$ and \bar{P}_K using $|M_A|^2$ obtained by Stephas and Crasemann [see Eq. (9) in Ref. 13]. As the Coulomb correction factor $F(Z+1, E_\beta)$, we used a conventional Fermi function. The shape factor for electron shakeoff during β decay, $S(E_\beta, E_0 - E_\beta^0)$, generally differs from that of ordinary β decay, $S(E_\beta, E_0 - E_\beta)$. However, since it is rather difficult to calculate $S(E_\beta, E_0 - E_\beta^0)$, we assumed these two shape factors to be equal, as done by other workers.¹³⁻¹⁵ For the case of ¹⁴⁷Pm, the factor for shakeoff can be set equal to unity under such an assumption, since the ordinary β spectrum of ¹⁴⁷Pm is of the allowed type. ⁶³Ni does not have an allowed-type spectrum, because it decays through an l -forbidden transition, but the shape factor has not been well studied. We were obliged to assume an allowed-type spectrum for this nuclide and set both $S(E_\beta, E_0 - E_\beta^0)$ and $S(E_\beta, E_0 - E_\beta)$ equal to unity for calculational simplicity. The antisymmetrization factor ϵ is $\frac{1}{4}$ for ¹⁴⁷Pm and $\frac{1}{2}$ for ⁶³Ni, respectively.

The calculated E_β^0 -dependent probability $P_K(E_\beta^0)$ is shown by solid curves in Figs. 8 and 9. These curves were drawn so as to fit the experimental results using the calculated values multiplied by constant factors (1.12 for ¹⁴⁷Pm and 0.95 for ⁶³Ni). The calculated total probability \bar{P}_K is also shown in the figures: 6.63×10^{-5} for ¹⁴⁷Pm and 3.47×10^{-4} for ⁶³Ni.

VI. DISCUSSION

As shown in Figs. 8 and 9, the experimental values of $P_K(E_\beta^0)$ determined for both ¹⁴⁷Pm and ⁶³Ni are in fairly good agreement with the calculated values in the whole energy region of E_β^0 , i.e., from near the K binding energy B_K to the β -transition energy limit E_0 , and the measured total probabilities \bar{P}_K for these nuclides agree also fairly well with the calculations. These results indicate strongly that the electron shakeoff process is the predominant mechanism of K -shell internal ionization, and an assumption of the sudden change of nuclear charge during β decay holds well even for very low energy β particles near B_K . Moreover, from our results it is concluded that the possible role of the direct-collision process suggested by Feinberg^{4, 10} can be neglected even in the low-energy region. According to his discus-

sion, if this process exists, behavior of the observed $P_K(E_\beta^0)$ would rise in this energy region.

Both measured and calculated probabilities $P_K(E_\beta^0)$ are nearly constant in the higher-energy region, but decrease rather steeply below about $2B_K$ and reach zero at B_K . According to the two-step treatment,¹² $P_K(E_\beta^0)$ should be independent of E_β^0 in the whole region. But, the conspicuous behavior of $P_K(E_\beta^0)$ in the low-energy region found by the present work indicates that electron shakeoff does occur as a one-step process. In the energy sharing of the electron shakeoff as a one-step process, the energies of most of the emitted K electrons, E_K , are relatively small, nearly equal to B_K or less. For this reason, it is expected that in the higher-energy region the spectrum of E_β^0 , $W_K(E_\beta^0)$ becomes the same as that of ordinary β decay, $W_\beta(E_\beta)$. This fact corresponds to the behavior of $P_K(E_\beta^0)$ being almost independent of E_β^0 in the high-energy region, and also to that of the composite electron spectrum measured by Fischbeck *et al.*¹⁵ using ¹⁴³Pr, which has a similar spectrum for the ordinary β decay in the higher-energy region. The noted decrease of $P_K(E_\beta^0)$ in the low-energy region can also be understood from the fact that E_K cannot be neglected in this region. It is worthy to note that in the recent experiment of orbital-electron shakeoff induced by external electrons, Carlson, Moddeman, and Krause²⁶ have observed a sharply decreasing probability in the low-energy region of impact electrons. Their observations are in accord with our observed behavior of $P_K(E_\beta^0)$. This fact may suggest that both β -induced shakeoff and impact-electron-induced shakeoff are under the control of the same mechanism.

The general behavior of $P_K(E_\beta^0)$ depends mainly on the value of B_K/E_0 . To examine this trend more closely, calculations of $P_K(E_\beta^0)$ have also been attempted for two nuclides with extreme values of B_K/E_0 : ¹⁴³Pr ($E_0 = 933$ keV, $B_K = 44$ keV) and ¹⁰⁷Pd ($E_0 = 35$ keV, $B_K = 26$ keV). The calculated results are shown in Fig. 10.

As mentioned in the preceding section, the β decay of ⁶³Ni is an l -forbidden transition with an unknown shape factor, but in the calculation of $P_K(E_\beta^0)$ we assumed an allowed-type spectrum. Fairly good agreement between calculated and experimental results, as shown in Fig. 9, sug-

gests that $P_K(E_\beta^0)$ may be almost independent of the type of the β transition involved. By assuming the shape factor for the electron shakeoff to be $S(E_\beta^0, E_0 - E_\beta^0)$ instead of $S(E_\beta, E_0 - E_\beta)$, $P_K(E_\beta^0)$ given by Eq. (13) can be seen to be independent of the transition type. Future experiments with β -decay nuclides having high forbiddenness are planned to judge which assumption is a better approximation; that is, our $S(E_\beta^0, E_0 - E_\beta^0) = S(E_\beta, E_0 - E_\beta)$, or $S(E_\beta, E_0 - E_\beta^0) = S(E_\beta, E_0 - E_\beta)$ as assumed by Stephas and Crasemann.¹³

Since in the region of very low E_β^0 an emitted β particle travels with slower velocity than that of a K electron in its orbit, the sudden approximation for the change in nuclear charge may no longer hold. In this case the adiabatic approximation would be proper. One can, therefore, expect that the experimental values of $P_K(E_\beta^0)$ in the region of E_β^0 near B_K would be less than that estimated by the present calculation using the sudden approximation.²⁷ However, such an expectation could not be verified by the present work. More exact

measurements in this region are planned to observe the small adiabatic effect.

As to the total ionization probability, other workers have compared their experimental values, in general, with the theoretical values calculated by the following equation derived from the simplest theory of electron shakeoff:

$$\bar{P}_K = 2 \int_0^\infty |M_A|^2 dE_K. \quad (15)$$

This equation is easily derived from our $P_K(E_\beta^0)$ expressed by Eq. (13) as an asymptotic case when $E_\beta^0 \rightarrow \infty$. When E_β^0 is much larger than B_K , we can approximate E_β^0 as to be nearly equal to E_β , and Eq. (13) can be reduced to

$$P_K(E_\beta^0 \gg B_K) = 2 \epsilon \int_0^\infty |M_A|^2 dE_K, \quad (16)$$

since in this case all other factors except $|M_A|^2$ in the integral in Eq. (13) can be set as unity. When the antisymmetrization between β particle and emitted K electron is neglected, i.e., $\epsilon = 1$, Eq. (16) becomes the same as Eq. (15). Therefore, Eq. (15) can be regarded as a very rough approximation of Eq. (14). It is noted here that in the measurement of the total ionization probability \bar{P}_K , only β particles with energies larger than B_K should be taken into account. The calculated results of \bar{P}_K for elements from $Z = 2$ to 92 based upon Eq. (15) with the use of self-consistent-field (SCF) wave functions have been published by Carlson, Nestor, Tucker, and Malik (CNTM).²⁸

In order to avoid confusion, it may be useful to add a further remark on the total ionization probability. As mentioned in Sec. II, the total ionization probability \bar{P}_K discussed in the present paper accounts for only β particles with energies larger than B_K , while the probability P_K by other workers except Erman *et al.*¹² accounts for all emitted β particles. In the present situation where the one-step process has been established in electron shakeoff, there seems to be no reason to adopt the probability \bar{P}_K defined by Eq. (3) as a total ionization probability of the process. Nevertheless, the probability \bar{P}_K is more reasonable than P_K when the probability calculated based on Eq. (15) using, for instance, the SCF wave functions is used for comparison between theory and experiment.

The experimental value of \bar{P}_K obtained by the present experiment, the theoretical values calculated by Eq. (14) using the relativistic hydrogenic wave functions, and those calculated by CNTM²⁸ using the SCF wave functions are listed in Table I. Both experimental and calculated values obtained by the present work show fairly good agreement.

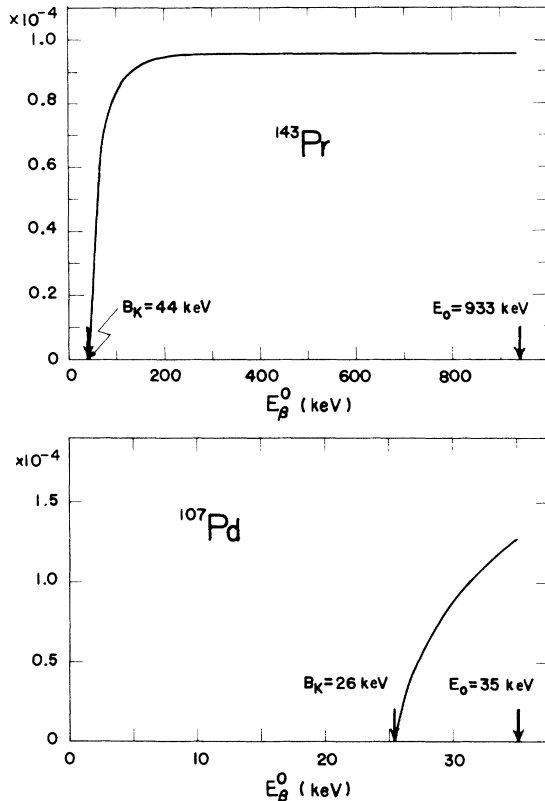


FIG. 10. Theoretical energy-dependent K -shell internal ionization probability $P_K(E_\beta^0)$ for ^{143}Pr and ^{107}Pd calculated by Eq. (13), based on the one-step electron shakeoff treatment. For ^{143}Pr (once parity forbidden) $\epsilon = \frac{1}{4}$, while for ^{107}Pd (assumed to be an allowed transition) $\epsilon = \frac{1}{2}$.

TABLE I. Total K -shell internal ionization probability per β decay, \bar{P}_K .

^{147}Pm	^{63}Ni	Method
$(7.6 \pm 1.1) \times 10^{-5}$	$(4.0 \pm 0.5) \times 10^{-4}$	Present measurement
6.63×10^{-5}	3.47×10^{-4}	Calculated from Eq. (14)
2.88×10^{-4}	1.15×10^{-3}	SCF calculations by Carlson ^a
5.15×10^{-5}	4.30×10^{-4}	SCF calculations, corrected

^aSee Ref. 28.

The SCF wave functions used by CNTM²⁸ are more reasonable than those used in the present work, but as one can see from the table, their values deviate considerably from our measured values. The total probability obtained by the SCF calculations should be improved by multiplying by a correction factor $\epsilon Q(B_K, E_0)$, where ϵ is the antisymmetrization factor and $Q(B_K, E_0)$ can be expressed by

$$Q(B_K, E_0) = \frac{\int_{B_K}^{E_0} W_K(E_\beta^0) [P_K(E_\beta^0) / P_K(E_\beta^0 \gg B_K)] dE_\beta^0}{\int_{B_K}^{E_0} W_K(E_\beta) dE_\beta} \quad (17)$$

By the use of the SCF calculations thus corrected, we obtained the theoretical values shown in the last row in Table I, which are in better agreement with our experimental values than those given by CNTM.²⁸ The expression of $Q(B_K, E_0)$ given by Eq. (17) is rather complicated. However, examining calculated results for many nuclides, it was found that Eq. (17) can be expressed approximately as

$$Q(B_K, E_0) \approx 1 - B_K/E_0. \quad (18)$$

Reviewing our work reported here, it is hoped that experiments with thinner sources than those used in these experiments can be attempted to obtain more exact information in the very low-energy region. Experiments with nuclides with larger B_K/E_0 , for instance ^{107}Pd , would be valuable. It is also hoped that more elaborate measurements of the total ionization probability \bar{P}_K for many different nuclides can be performed to provide more meaningful comparisons with theory, although many experimental results have so far been published. A triple-coincidence measurement between K x ray, β particle, and K electron using ^{147}Pm is now in progress.

ACKNOWLEDGMENTS

We want to express our thanks to Yasuyuki Nakayama, Shoji Isozumi, and Tetsuo Kitahara for their cooperation in the experimental work, and to Dr. Takeshi Mukoyama for valuable discussions. We are also very grateful to Dr. M. S. Freedman of the Argonne National Laboratory for many helpful comments and for communicating the interesting work by his group prior to publication.

- ¹E. L. Feinberg, *J. Phys. (USSR)* **4**, 423 (1941).
²A. Migdal, *J. Phys. (USSR)* **4**, 449 (1941).
³F. Boehm and C. S. Wu, *Phys. Rev.* **93**, 518 (1954).
⁴H. Langevin-Joliot, *Ann. Phys. (Paris)* **2**, 16 (1957).
⁵G. A. Renard, *J. Phys. Radium* **18**, 681 (1957).
⁶G. Charpak and F. Suzor, *J. Phys. Radium* **20**, 31 (1959).
⁷F. Suzor and G. Charpak, *J. Phys. Radium* **20**, 647 (1959).
⁸F. Suzor and G. Charpak, *J. Phys. Radium* **20**, 25 (1959).
⁹M. Spighel and F. Suzor, *Nucl. Phys.* **32**, 346 (1962).
¹⁰E. L. Feinberg, *Yadern. Fiz.* **1**, 612 (1965) [transl.: *Soviet J. Nucl. Phys.* **1**, 438 (1965)].
¹¹R. M. Weiner, *Phys. Rev.* **144**, 127 (1966).
¹²P. Erman, B. Sigfridsson, T. A. Carlson, and K. Fransson, *Nucl. Phys.* **A112**, 117 (1968).
¹³P. Stephan and B. Crasemann, *Phys. Rev.* **164**, 1509 (1967).
¹⁴B. Crasemann and P. Stephan, *Nucl. Phys.* **A134**, 641 (1969).
¹⁵H. J. Fischbeck, F. Wagner, F. T. Porter, and M. S. Freedman, *Phys. Rev. C* **3**, 265 (1971).
¹⁶R. S. Mowatt and J. S. Merritt, *Can. J. Phys.* **48**, 453 (1970).
¹⁷P. Gorenstein and S. Mickiewicz, *Rev. Sci. Instr.* **39**, 816 (1968); J. L. Campbell, *Nucl. Instr. Methods* **65**, 333 (1968); G. F. Snelling, United Kingdom Atomic Energy Research Group Report No. AERE-R 5749, 1968 (unpublished); L. L. Lewyn, *Nucl. Instr. Methods* **82**, 138 (1970).
¹⁸Y. Isozumi and S. Isozumi, to be published.
¹⁹E. A. Wolicki, R. Jastrow, and F. Brooks, U. S. Naval Research Laboratory Report No. 4833, 1956 (unpublished); R. L. Heath, U. S. Atomic Energy Commission Report No. IDO-16880-1, 1964 (unpublished).
²⁰W. F. Miller, J. Reynolds, and W. J. Snow, Argonne National Laboratory Report No. ANL-5902, 1958 (unpublished).
²¹C. M. Davison, in *Alpha-, Beta-, and Gamma-Ray Spectroscopy*, edited by K. Siegbahn (North-Holland Publishing Company, Amsterdam, The Netherlands, 1965), Vol. 1, Appendix 1.
²²J. R. Dell and P. J. Ebert, *Nucl. Instr. Methods* **68**,

335 (1969).

²³V. O. Kostroun, M. H. Chen, and B. Crasemann, *Phys. Rev. A* **3**, 533 (1971).

²⁴The authors are grateful to Dr. M. S. Freedman for pointing out this fact.

²⁵C. F. Schwerdtfeger, H. J. Prask, and J. H. Mihelich, *Nucl. Phys.* **35**, 168 (1962).

²⁶T. A. Carlson, W. E. Moddeman, and M. O. Krause, *Phys. Rev. A* **1**, 1406 (1970).

²⁷From the comparison between the measured energy-dependent probability and its calculated values for ¹⁶³Er and ²¹⁰Bi, Erman *et al.* (Ref. 12) pointed out that the sudden approximation may no longer hold in the low-energy region. However, this indication was derived from their semitheoretical calculations based on the two-step treatment.

²⁸T. A. Carlson, C. W. Nestor, Jr., T. C. Tucker, and F. B. Malik, *Phys. Rev.* **169**, 27 (1968).

PHYSICAL REVIEW C

VOLUME 4, NUMBER 2

AUGUST 1971

(³He,*d*) Reaction to Bound and Quasibound Levels in ⁹³Tc[†]

R. L. Kozub and D. H. Youngblood

Cyclotron Institute, Texas A & M University, College Station, Texas 77843

(Received 1 March 1971)

The ⁹²Mo(³He,*d*)⁹³Tc reaction has been studied at 35-MeV bombarding energy. Several $T_{<}$ levels are observed below 6-MeV excitation energy, and evidence is presented for sizable $p_{3/2}^{-2}$ and $f_{5/2}^{-2}$ components in the ⁹²Mo proton configuration. Four deuteron groups, corresponding to $T_{>} = \frac{3}{2}$ analogs of low-lying levels in ⁹³Mo are also observed. Distorted-wave Born-approximation calculations were performed, using form factors calculated for a proton quasibound by the Coulomb and centrifugal barrier for the proton-unstable levels (≥ 4.08 -MeV excitation energy). The data are well described by the calculations, and reasonable spectroscopic factors are obtained for both $T_{<}$ and $T_{>}$ levels.

I. INTRODUCTION

The structure of nuclei in the $A = 90$ region has been studied quite extensively both theoretically and experimentally. The models used to describe the proton configurations for $Z \geq 39$ in the presence of the $N = 50$ closed shell are usually based on a ⁸⁸Sr or ⁹⁰Zr closed core,¹⁻³ and studies of low-lying levels in this region via proton transfer reactions⁴⁻⁷ appear to have verified this assumption. We have studied the ⁹²Mo(³He,*d*)⁹³Tc reaction up to 11-MeV excitation energy to investigate the proton configuration of the ⁹²Mo ground state and the nature of the $T = \frac{3}{2}$ isobaric analog states (IAS), which are also excited in this reaction. Ohnuma and Yntema⁴ and Picard and Bassani⁵ (referred to as PB in the following discussions) have also studied some of the low-lying $T_{<}$ levels with the ⁹²Mo(³He,*d*)⁹³Tc reactions; however, no analysis was made of levels above the ⁹³Tc proton separation energy (4.08 MeV). We have performed distorted-wave Born-approximation (DWBA) calculations for the proton-unstable $T_{<}$ and $T_{>}$ states, using a technique reported previously⁸ for the analysis of stripping to unbound levels.

II. EXPERIMENTAL PROCEDURE AND RESULTS

A 35.0-MeV ³He beam from the Texas A & M cyclotron was used to bombard a 1.10-mg/cm² self-

supporting Mo foil enriched to 98.3% in ⁹²Mo. The beam was focused to a 3-mm-diam spot at the center of the 30-in. scattering chamber and collected in a Faraday cup 2 m behind the chamber. A beam-energy spread of ~35 keV was obtained through the use of the $n = \frac{1}{2}$ analyzing magnet. A ΔE - E detector telescope consisting of a 1-mm-thick ΔE detector and a 3-mm-thick E detector was used to detect the deuterons and the elastically scattered helium ions simultaneously. The beam axis in the scattering chamber was located to within 0.1° by rotating the detector into the "beam" resulting from the few ions produced in the cyclotron with no ion-source arc current and a small filament current. A detector fixed at 35° was used to monitor the current integrator.

Pulses from the ΔE and E detector were routed past time pickoffs and through amplifiers to a power-law identifier circuit where deuteron pulses were selected. The total energy ($E + \Delta E$) pulses were fed through a biased amplifier and stretcher to an analog-to-digital converter which was interfaced to the IBM 7094 computer. The spectra (1024 channels each) were stored in the computer memory and transferred to magnetic tape at the end of each run. Also, four spectra from previous runs were retained in the memory, and the data were reduced on line to absolute, center-of-mass cross sections with the aid of the display oscillo-